Biomass Conversion and Biorefinery (2024) 14:9653–9666
https://doi.org/10.1007/s13399-022-03096-7

ORIGINAL ARTICLE

Influence of aging on the rheological behavior and characteristics of bio-oil produced from olive pomace via slow pyrolysis

Ahmed Ayyash[1] · Esin Apaydın Varol[1] · Murat Kılıç[1] · Gamzenur Özsin[2]

Received: 23 April 2022 / Revised: 29 June 2022 / Accepted: 17 July 2022 / Published online: 29 July 2022

Abstract

Biomass-derived pyrolytic oil, bio-oil, has the potential to substitute fossil fuels from a sustainable point of view. The utilization of bio-oil in different applications is limited due to the aging effects on its stability in terms of its compositional, thermal, and rheological changes. Thus, the objective of this work is to investigate the short- and long-term storage effects on bio-oil properties. For this purpose, bio-oil produced from olive pomace using a laboratory-scale slow pyrolysis reactor was aged under two different conditions: at room temperature in a sealed bottle for 7 days and under accelerated aging conditions (80 °C) for 24 and 168 h. The raw and aged bio-oil samples were characterized by elemental analysis, thermogravimetric analysis (TGA), gas chromatography–mass spectrometry (GC–MS), Fourier transform infrared spectroscopy (FT-IR), TGA-FT-IR, and rheometer. Carboxylic acids, esters, and phenols were detected to be the main groups of bio-oil. Long-term and high-temperature storage, known as accelerated aging, affected the rheological behavior of bio-oil while increasing the instability, which is attributed to the polymerization reactions that occurred during storage. The viscosity of this aged bio-oil was measured as 111.2 cP at 20 °C, which is 46.8% higher than that of the fresh bio-oil. The maximum decomposition temperature was shifted to around 300 °C for the 168 h of accelerated aged bio-oil. Overall, this study enables a better understanding of the olive pomace-based bio-oil storage conditions for its possible use as a synthetic fuel and provides data for the development of more feasible biorefinery processes.

Keywords Olive pomace · Bio-oil · Viscosity · Slow pyrolysis · Rheology · Stability

1 Introduction

Due to environmental concerns such as sustainability, atmospheric carbon accumulation, and the associated global warming, seeking new alternative and clean energy sources to fossil fuels becomes inevitable [1–3]. At this point, biomass, as a widely available renewable energy resource, has a great potential to partially substitute fossil fuels [4, 5]. Biomass includes abundant sugar polymers labile to be converted into specialty chemicals, and hence, it is considered an ideal feedstock for sustainably renewable energy applications [6]. To date, various thermochemical conversion processes have been applied for converting biomass into synthetic fuels. Among these processes, pyrolysis has caught increasing attention for its ability to produce environmentally safe and renewable fuels via simple, low-cost, and flexible thermal degradation [7, 8].

Basically, the biomass pyrolysis process is an endothermic decomposition implemented in an oxygen-deficient environment to obtain bio-oil, syngas, and biochar. A variety

Highlights
- The thermal and long-term storage stability of bio-oil was investigated.
- Thermogravimetry, spectroscopy, and chromatography were used for characterization.
- Bio-oil mainly contained carboxylic acids (~58%) and phenolics (~16%).
- Rheological behavior was determined by shear rate and temperature ramp tests.
- The aging index was calculated at different temperatures.

✉ Esin Apaydın Varol
eapaydin@eskisehir.edu.tr

[1] Department of Chemical Engineering, Faculty of Engineering, Eskisehir Technical University, Eskişehir 26555, Turkey

[2] Department of Chemical Engineering, Faculty of Engineering, Bilecik Şeyh Edebali University, Bilecik 11230, Turkey

of biomass sources can be used as feedstock for pyrolysis processes such as plant-based materials (crops and agricultural residue), industrial waste, and municipal solid waste [9, 10]. The subtle point to consider during biomass selection for pyrolysis is the abundance and continuity of the feedstock. In this perspective, olive oil pomace as a waste stream of the oil industry can be considered a suitable biomass material, especially for the Mediterranean countries. It is known that olive is one of the main agricultural products in the Mediterranean region with more than 95% of olive oil production worldwide. Approximately 17 million tons of grain olives are obtained from 900 million olive trees in around 10 million hectares of land in the world. The average worldwide annually olive oil production, according to the last 5 seasons, is around 3.2 million tons/year [11]. Spain, Italy, Tunisia, Greece, and Turkey are the most olive producers in the world, both in terms of land devoted to olive tree cultivation and olive oil production [12]. Moreover, a life cycle assessment study on olive pomace valorization showed that pyrolysis process is an ecological tool using energy-efficient equipment [13]. Olive pomace is the main residue of the olive oil extraction process that is a thick dark brown sludge. It is the remaining pulpy material after removing most of the oil from the olive paste, and it consists of pieces of skin, pulp, stone, and olive kernel [14–16]. In the structure of olive pomace, a variety of compounds of carbohydrates, lipids (remaining oil), phenols, and inorganics exist. Cellulose, hemicellulose, and lignin are known to be the main biochemical components of the pomace; however, fatty oils and protein are also present in significant quantities [14, 16–18]. The findings of the previous studies verify that the olive pomace has considerable potential for efficient biorefinery processes since its bio-oil has similar characteristics to petroleum fractions with a suitable calorific value [14, 19–23].

During biomass pyrolysis, a complex mixture of hydrocarbons is formed due to the non-synchronized decomposition of biomass constituents, namely cellulose, hemicellulose, and lignin [24, 25]. Therefore, bio-oil includes a large number of organic substances in its structure, such as ketones, aldehydes, alkanes, acids, alcohols, esters, anhydrosugars, furans, phenols, guaiacols, syringols, and aromatic compounds together with water and large molecular oligomers [26]. Due to this complex structural composition of bio-oil, it exhibits some unfavorable properties like high acidity, high moisture content, and poor stability which limits its widespread applications for heat and power generation and applications in the chemical industry [27–29]. Furthermore, the components of bio-oil may react with each other, forming macromolecular organics, which eventually cause bio-oil aging during storage. As a result of the instability of bio-oil, viscosity increment is observed during storage, especially if exposed to relatively high temperatures [30]. It is well-known that aging not only deteriorates the quality of bio-oil but also influences the refining of bio-oil and its extracted chemicals since it causes obvious changes in the physical and chemical properties [31]. Therefore, the stability of bio-oils needs to be studied in detail during their use.

By far, although various process parameters on olive pomace pyrolysis product yields have been investigated such as temperature [21], heating rate [32], heating type [19], residence time [34], catalysis [35, 36], pressure [37, 38], and pyrolysis atmosphere [20] together with effects of pretreatment [14, 23, 39], the intrinsic effect of aging on olive pomace-based bio-oil characteristics has not been studied yet. On the other hand, there have been several studies over the years measuring the stability of pyrolytic liquid from different biomasses, but none of them studied the thermal and rheological behavior of bio-oil produced from the olive pomace, or no viscosity measurements were carried out at specific temperatures and a specific shear rate or a narrow shear rate range. A few papers have been reported on the storage stability of pyrolytic bio-oil. Diebold reported a review that focused on bio-oil storage instability and the possible chemical reactions taking place during storage [40]. Cai et al. provided a study that investigated long-term (2 years) storage on rice husk pyrolytic liquid under three different conditions and concluded that the low storage temperatures slowed down the degradation reactions [27]. In another study, both accelerated aging and long-term storage on torrefied wood pyrolytic liquid physicochemical and compositional properties were investigated [41]. Having focused on the scientific essence of the aforementioned issue, the effect of storage and aging seems to require being resolved for efficient and feasible bio-oil utilization. Considering the high-temperature performance and aging resistance required for many engineering applications, improvement in the rheology can give a more detailed performance-related characterization with varying degrees of aging to qualitatively verify the consistency in general characteristics. Therefore, this study aims to investigate the effect of different storage conditions on bio-oil thermal and storage stability in terms of rheological and analytical characterization techniques. In this way, important fundamental data about the performance and characteristics of olive pomace-based bio-oil will constitute an important resource for further engineering applications.

2 Materials and methods

2.1 Raw material

The olive oil pomace (olive residue) used in this study as feedstock was collected from Manisa city located in the

Aegean Region, west of Turkey, during the 2019 season. Olive pomace consisted of the solid remains of the olive including skins, pulp, seeds, and stems. The feedstock was dried at room temperature for a few days before pyrolysis to extract any excess water content. The main characteristics of olive pomace are listed in Table 1.

2.2 Raw material characterization

2.2.1 Thermogravimetric analysis

The thermogravimetric analysis was carried out using Setaram Labsys-Evo to investigate the thermal decomposition behavior of the raw material. The sample was heated from room temperature to 1000 ℃ in N_2 atmosphere with a flow rate of 20 ml.min^{-1}, at a heating rate of 10 °C.min^{-1}.

2.3 Bio-oil production via pyrolysis

Pyrolytic oil was obtained from olive pomace via slow pyrolysis using a fixed bed reactor details of which was given in the previous studies [42]. The reactor was fixed in an electrically heated oven to obtain the desired pyrolysis temperature. The reactor temperature was maintained at 500 °C using a PID controller with a K-type thermocouple placed on the top of the reactor. After the reactor was filled with feedstock, its upper chamber was sealed carefully to ensure that there are no gas leakages. The final temperature of the reactor was set to 500 °C at a heating rate of 10 °C.min^{-1}. After reaching the final temperature, a holding period of 15 min was sustained. The volatiles produced during pyrolysis were swept out using nitrogen that flows in the reactor at 100 cm^3.min^{-1} and passed through four cylindrical bio-oil traps placed in an ice bath. The condensed volatiles were collected as bio-oil with a certain amount of water, which was further separated. The difference in the density of water and bio-oil makes it simple to separate them using a standard separation funnel. Bio-oil having a density lower than the water creates a two-phase liquid in the funnel where the bio-oil is the upper phase and the water was drained slowly from the bottom. The water-free, fresh bio-oil was transferred to a closed glass vessel and kept in the refrigerator at 4 °C for further analyses. All analyses for fresh bio-oil were carried out using the bio-oil without any treatment except water separation.

Table 1 Main characteristics of the biomass

		Ratio (wt.%)	Method
Proximate analysis	Moisture	7.1	ASTM D2016-74
	Ash	3.4	ASTM D1102-84
	Volatile	82.3	ASTM E897-82
Ultimate analysis	C	59.45	ASTM D 5373
	H	6.96	ASTM D 5373
	N	5.37	ASTM D 5373
	O*	28.22	
	H/C	0.12	
	O/C	0.47	

* By difference

2.4 Bio-oil aging

Bio-oil samples were aged under two different conditions: (i) at room temperature for 7 days and (ii) at 80 °C, known as accelerated aging, for 24 and 168 h. In the literature, accelerated aging refers to 24 h of storage at 80 °C, and it is reported to be equivalent to 1 year of storage at room temperature [43, 44]. Therefore, in this study, both short- and long-term aging were performed to investigate the effects of storage time on the characteristics of bio-oil. Bio-oil samples are named as follows: "fresh" for the bio-oil before the aging; "7-day aged" for the samples aged at room temperature for 7 days; and "24-h accelerated aged" and "168-h accelerated aged" for the samples aged at 80 °C for two different durations. During aging, all samples were placed in separate brown-colored glass bottles, which were tightly closed and stored in a dark environment.

2.5 Bio-oil characterization

The elemental composition, C, H, and N, of each sample, was determined using a LECO CHN628 elemental analyzer using ASTM D-5377 method. Oxygen content was calculated by difference (100% – ($C+H+N$)). The determination of the calorific value of bio-oil samples was accomplished by using the Dulong equation [16]:

$$Q_{GCV}\left(\frac{MJ}{kg}\right) = 33.83C + 144.3\left(H - \frac{O}{8}\right) \quad (1)$$

where C, H, and O are the mass fractions of carbon, hydrogen, and oxygen, respectively, and Q_{GCV} is the gross calorific value in MJ.kg^{-1}.

Fourier transform infrared spectroscopy (FT-IR) was used to analyze the organic functional groups in the bio-oil samples before and after the aging process. A Thermo Fisher Scientific Nicolet iS10 FT-IR spectrometer with a resolution of 4 cm and 32 scans was used for analyzing samples between 4000 and 500 cm^{-1}. With the OMNIC software, spectral analysis was done and reproducibility and accuracy of the gained data were confirmed.

The gas chromatography–mass spectroscopy (GC–MS) analysis was carried out on each sample using Agilent Technologies 7820A Gas Chromatography (GC)–5977B Mass Spectroscopy (MS) equipped with

30 m × 0.25 mm × 0.25 µm HP-5MS column. The temperature of the GC oven was programmed to hold at 40 °C for 3 min, and then, the temperature was increased at a rate of 2 °C.min^{-1} to hold for 30 min after reaching the final temperature of the oven set as 270 °C. A 1-µL sample injection was adopted. Helium flow rate was adjusted as 1 mL/min. W9N11 mass spectral library was used to identify the obtained peaks.

Thermogravimetric analysis (TGA) experiments were carried out using Labsys Eyo (SETARAM Instrumentation), and the gases that evolved during thermal decomposition were detected by a simultaneous FT-IR (Thermo-Nicolet IZ10). Approximately 10 ± 1.0 mg of sample was loaded into a 100 µL alumina crucible and heated from 25 to 1000 °C with a heating rate of 20 °C.min^{-1} where 20 mL/min nitrogen was used as the sweeping gas. Before each analysis, a blank experiment was performed and subtracted from the TGA data of the samples to eliminate the systematic errors of the instrument. During pyrolysis, evolved gases were swept through the capillary transfer lines which were connected to the FT-IR spectrometer. To avoid condensing, the transfer line and FT-IR cell were maintained at 225 °C and 250 °C, respectively. FT-IR spectra were recorded from 4000 to 400 cm^{-1} using OMNIC software.

All characterization tests were applied to fresh and aged samples, and to ensure the accuracy of the experimental results, all the experiments were conducted at least twice.

2.6 Rheology

The dynamic viscosity of bio-oil samples was determined by using Kinexus ultra + (Malvern UK) rheometer. Two different tests were applied to each sample, shear rate ramp and temperature ramp. Shear rate ramp tests were applied between 5 and 580 s^{-1} to each sample at different temperatures of 20, 25, 30, 35, and 40 °C. To reach a steady state at the target temperature, 5 min of holding time was applied.

Temperature ramp tests were applied between 20 and 60 °C to each sample with a 1 °C.min^{-1} heating rate at constant shear stress (1 Pa). The temperature is controlled using an active hood Peltier plate cartridge with ± 0.01 °C temperature resolution and ± 0.1 °C temperature stability; this cartridge is designed for accurate measurement of samples with volatile components and to minimize sample drying. The experimental error in viscosity measurements was found to be less than 2.45% by using standard mineral oil. Cone plate stainless steel geometry was used with a 40 mm diameter and 4° angle because this geometry requires a small sample volume and generates a homogeneous shear field on the sample compared to different geometries. During the tests, the cone plate gap was 0.1498 mm, and ~ 1.2 mL volume of sample was required. The data was gathered using rSpace and was analyzed using OriginPro 9.0.0 software.

The change in the dynamic viscosity, $\Delta\eta$, known as the aging index was calculated using the following equation [35, 38]:

$$\Delta\eta = \frac{\eta_{Aged} - \eta_{Fresh}}{\eta_{Fresh}} \times 100\% \quad (2)$$

3 Results and discussion

3.1 Thermal decomposition behavior of olive pomace and bio-oil production

Pyrolysis experiments were carried out at 10 °C/min under nitrogen by TGA. The TG and DTG curves are shown in Fig. 1. The main pyrolysis reactions started around 170℃ and completed at 560℃, giving a maximum decomposition rate of 6.4%/min at 322℃. The total mass loss was recorded as 77.4 wt.%. According to the thermal decomposition data, the pyrolysis temperature to produce bio-oil is selected to be 500 ℃ for the further bench-scale experiments.

Slow pyrolysis was applied at this temperature under an inert atmosphere to avoid secondary reactions. The bio-oil yield was achieved to be around 35 wt. %, which is consistent with the previous studies [20, 21]. For instance, Uzun et al. studied the fast pyrolysis of olive pomace at different pyrolysis temperatures and retention times. According to their results, the highest bio-oil yield of 46.7 wt.% was achieved at 500 °C when the heating rate was 500 °C.min^{-1} [16]. For the case of slow pyrolysis, on the other hand, the bio-oil formation was reported to be significantly lower with a yield of wt. 37.7% at the same temperature [45].

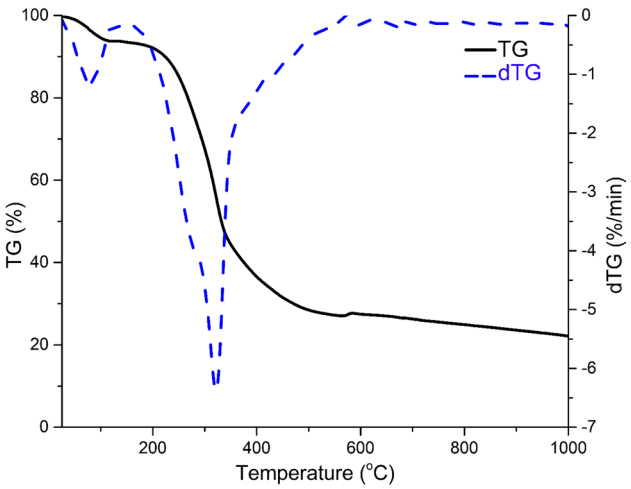

Fig. 1 Thermal decomposition behavior of olive pomace

3.2 Bio-oil characterization

3.2.1 Elemental composition

The ultimate analysis results of bio-oil samples are given in Table 2. The analyses showed that all bio-oil samples contained almost the same percentages of carbon, hydrogen, nitrogen, and oxygen. All results were in the accuracy range specified by the standard materials used for calibration. Aged bio-oil samples were carefully sealed to prevent any contact with air/oxygen to prevent or minimize oxidation reactions. As a result, the oxygen content of aged bio-oil samples showed minor changes with respect to that of fresh bio-oil samples. Separating bio-oil from water content immediately after pyrolysis resulted in higher carbon and lower oxygen contents compared to other studies [21]. However, still, the oxygen content of bio-oil is around 15 wt. %, which is one of the main problems of bio-oil utilization as an alternative to petroleum-derived oils. The increased content of oxygen results in a lower energy density and also accelerates the oxidative degradation reactions during the storage time. Moreover, the oxygenated chemical compounds are highly reactive and promote the instability of the bio-oil [46, 47]. The ratios of atomic hydrogen and oxygen to carbon (H/C and O/C) are critical indicators of calorific value and stability. The biofuels with a high H/C ratio have higher calorific values, while the lower O/C ratio specifies better fuel stability. The higher the calorific value is, the closer the bio-oil to the synthetic fuel. As seen in Table 2, the average gross calorific value of bio-oil samples was calculated as 35.74 $MJ.kg^{-1}$, which is close to that of petroleum products [48] and higher than that of typical bio-oil samples [49] due to separation of water from the oil fraction immediately after pyrolysis.

Table 2 Elemental analysis results of fresh and aged bio-oil samples (as received, wt. %)

	Fresh	7 days aged	24-h accelerated aged	168-h accelerated aged
C	73.36	74.05	73.74	73.40
H	9.34	9.26	9.44	9.39
N	2.17	2.20	2.23	2.16
O*	15.13	14.49	14.60	15.05
H/C	1.52	1.49	1.53	1.52
O/C	0.16	0.15	0.15	0.15
Q_{GCV}** (MJ/kg)	35.56	35.80	35.93	35.67

* By difference

** Gross calorific value

3.2.2 Functional groups of bio-oil samples

The functional groups of bio-oil samples were detected by FT-IR spectroscopy (Fig. 2), and the summary of the main functional groups detected by FT-IR is summarized in Table 3. During the aging process, although a series of reactions took place, all major bands attributed to similar functional groups are observed in the spectra due to the negligible change in the composition of bio-oil. Moreover, the presence of oxygenated compounds is observed from the spectra through the carboxyl and carbonyl group vibration bands.

The O–H stretching vibrations between 3200 and 3570 cm^{-1} observed in all FT-IR spectra indicate the presence of hydroxyl groups in alcohols and phenols. The weak peaks at around 3010 cm^{-1} are related to the aromatic = C-H vibrations from the aromatic ring [50]. The symmetric and asymmetric stretching vibration associated with the peaks at around 2925 and 2854 cm^{-1} of C-H is attributed to methyl and methylene groups. The only difference between the fresh and aged bio-oil samples is the relative intensities and sharpness of these vibration bands. The C = O group is arising mainly from the aldehydes, ketones, and carboxylic acids, and the stretching bands are observed between 1685 and 1760 cm^{-1}. The strong peak at 1711 cm^{-1} observed for all samples is assigned to the stretching vibrations of carboxylic acid, which is a common characteristic of edible oil and is further confirmed by GC–MS analysis [51]. The 1340–1470 cm^{-1} C–H bending vibrations correspond to alkyl and aliphatic groups. The stretching vibrations associated with the peaks at 1242 and 1264 cm^{-1} are likely indicative of C–O stretching vibration in organic acids, ethers, and alcohol groups. The presence of –OH groups is confirmed by

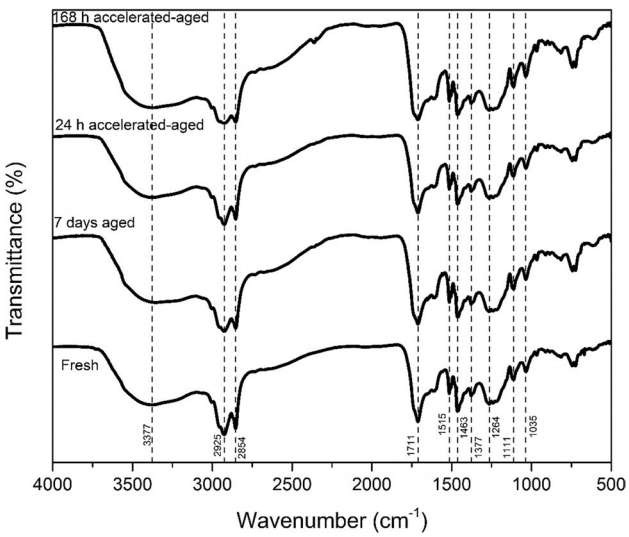

Fig. 2 FT-IR spectra of bio-oil samples

Table 3 The main functional groups of bio-oil

Wavenumber (cm^{-1})	Functional group	Compounds
3200–3570 (broad)	O–H (stretching)	Hydrogen-bonded alcohols, phenols
3000–3100	C-H (stretching)	Aromatic rings
2850–2970	C-H (stretching)	CH_2 or CH_3 groups
1690–1760	C = O (stretching)	Aldehydes, ketones, carboxylic acids
1500–1600	C = C (stretching)	Aromatic rings
1340–1470	C-H (bending)	Alkyl, aliphatic
1050–1300	C-O (stretching)	Alcohols, ethers, carboxylic acids
1000–1200	C-H (bending)	Aromatic rings
1000–1060	C-O (stretching)	Ethers, alcohols, phenols

the stretching vibrations of C–OH at 1110 cm^{-1}. The stretching vibrations between 1060 and 1030 cm^{-1} are attributed to stretching vibrations of C-O belonging to the carboxyl (-COOH) group [21, 50, 52].

3.2.3 GC–MS analysis

GC–MS analysis provides information about the components of bio-oil samples to understand the changes in the composition due to the possible chemical reactions during the aging period. According to GC–MS spectra and library search results, bio-oil is a complex mixture of hydrocarbons, containing more than 100 compounds. To eliminate the inaccuracies, only the components with relatively high matching quality (higher than 50) were selected in this study and classified as phenols, carboxylic acids, alkanes, ketones, esters, alcohols, aldehydes, and aromatics. The distribution of the fresh and aged bio-oil compounds that are identified according to the retention times is given in Table 4. The majority of fresh bio-oil is oleic acid with the highest relative percentage of 46.80%, which is a kind of fatty acid and grouped in carboxylic acids. The phenolic compounds have the second major contribution to bio-oil composition. It is known that the lignocellulosic biomass is oxidized to phenols during the pyrolysis process, and hence, fresh and aged bio-oil produced from olive pomace has approximately 17% phenolic compounds [20, 53]. Due to the presence of these high fractions of oxygenated compounds, i.e., fatty acids, the stability of bio-oil is low, and a free-radical chain reaction, namely, autoxidation reaction, occurs during the long-term storage [54]. To prevent the formation of free radicals, it is necessary to keep the bio-oil under inert conditions. In this study, the bio-oil samples were aged in closed vessels, and therefore, the possible oleic acid decomposition reactions were minimized. To precisely observe the effect of aging on the composition of bio-oil, the variations in the areas of each component group are demonstrated in Fig. 3. For the fresh bio-oil, the main groups were carboxylic acids, phenolics, and esters with percentages of 58.4, 16.8, and 16.5, respectively. After aging, it is noticed that the percentage of carboxylic acids decreased slightly by ~ 10% to 53% when 168-h accelerated aging was applied. On the other hand, esters, ketones, and aromatics percentage areas slightly increased. The possible explanation for this substitution is the esterification reactions, where the –OH group of the carboxylic acid is replaced by –OR' groups to give esters. Moreover, the fraction of aromatic compounds in the fresh bio-oil represents 2.5%, and it increased to 3.3% after 168-h of accelerated aging. The dehydrogenation of existing cyclic compounds during the storage resulted in an increase in the aromatic compounds, which also increased the higher molecular weight hydrocarbon fractions. The results are consistent with the previous studies as Grioui et al. reported that hydroxyl, carbonyl, and carboxyl group components are the main reactants for the chemical reactions that occurred during storage [51].

3.2.4 Thermal decomposition behavior of bio-oil

The thermal stability of fresh and aged bio-oil samples is indicative of their rheological behavior. Figure 4 shows the weight loss of bio-oil samples during thermal decomposition at a 20 °C/min heating rate, and Table 5 summarizes the decomposition temperatures. It is seen that around 93 wt. % of the samples were decomposed at the final temperature of 1000 °C and all bio-oil samples exhibited almost the same mass loss. The decomposition of bio-oil was accomplished in a single step between around 45 and 510 °C. Lower molecular weight hydrocarbons such as aldehydes, alcohols, and carboxylic acids were volatilized at temperatures between 45 and 130 °C, and when the temperature increased to around 130 °C, complex pyrolysis reactions started to take place resulting in rapid degradation. The TG curves of the aged samples shifted to the right due to the formation of a higher molecular weight tar sample during the aging process as a result of the polymerization reactions. Figure 4 also shows dTG curves for each sample; the maximum decomposition rate increased by 17 °C from 281 °C for fresh bio-oil to 298 °C for 168 h of accelerated aged bio-oil. The main decomposition occurred in a single step, followed

Table 4 GC–MS results for fresh and aged bio-oil samples

Compounds	Molecular formula	Area (%)			
		Fresh	7 days	24 h	168 h
Alcohols					
2-Furanmethanol	$C_5H_6O_2$	0.17	0.38	0.36	0.31
Aldehydes					
9-Tetradecenal, (Z)-	$C_{14}H_{26}O$	–	0.80	–	0.81
Alkanes					
Octane	C_8H_{18}	0.22	0.15	0.21	0.19
Nonane	C_9H_{20}	0.18	0.20	0.16	0.14
Decane	$C_{10}H_{22}$	–	0.26	0.16	0.15
Undecane	$C_{11}H_{24}$	–	0.24	0.23	0.30
Dodecane	$C_{12}H_{26}$	–	0.26	0.27	0.26
Tridecane	$C_{13}H_{28}$	–	0.36	0.29	0.27
Tetradecane	$C_{14}H_{30}$	0.31	0.32	0.34	0.32
Pentadecane	$C_{15}H_{32}$	0.46	0.48	0.46	0.45
Hexadecane	$C_{16}H_{34}$	–	0.27	0.27	0.25
Aromatics					
Toluene	C_7H_8	0.45	0.41	0.34	0.30
Ethylbenzene	C_8H_{10}	0.18	–	–	–
Benzene, 1,3-dimethyl-	C_8H_{10}	0.16	0.13	0.13	0.12
Styrene	C_8H_8	0.05	0.12	0.11	0.09
p-Xylene	C_8H_{10}	0.20	0.19	0.18	0.15
2,4,6-Octatriene, 2,6-dimethyl-	$C_{10}H_{16}$	–	0.19	0.25	0.25
2,3,5-Trimethoxytoluene	$C_{10}H_{14}O_3$	–	–	–	1.01
Squalene	$C_{30}H_{50}$	1.47	1.42	1.43	1.36
Carboxylic acids					
3,5-Dimethoxy-4-hydroxyphenylacetic acid	$C_{10}H_{12}O_5$	0.18	0.25	0.11	0.11
Oleic acid	$C_{18}H_{34}O_2$	46.80	41.94	44.46	42.55
n-Hexadecanoic acid	$C_{16}H_{32}O_2$	11.39	12.43	9.75	10.30
Ester					
Hexadecanoic acid, methyl ester	$C_{17}H_{34}O_2$	2.53	2.36	2.51	2.54
9,12-Octadecadienoic acid (Z,Z)-, methyl ester	$C_{19}H_{34}O_2$	1.06	1.10	1.04	1.07
9-Octadecenoic acid, methyl ester	$C_{19}H_{36}O_2$	12.95	11.75	12.36	12.74
9-Octadecenoic acid (Z)-, 2,3-dihydroxypropyl ester	$C_{21}H_{40}O_4$	–	1.02	1.10	1.08
Ketones					
2-Cyclopenten-1-one, 2-methyl-	C_6H_8O	–	0.19	0.17	0.15
Butyrolactone	$C_4H_6O_2$	0.21	0.24	0.22	0.20
2-Cyclopenten-1-one, 2-hydroxy-3-methyl-	$C_6H_8O_2$	–	0.43	0.25	0.42
2,4-Dihydroxypropiophenone	$C_9H_{10}O_3$	–	0.12	0.14	0.13
2-Propanone, 1-(4-hydroxy-3-methoxyphenyl)-	$C_{10}H_{12}O_3$	0.46	0.44	0.42	0.47
Phenols					
Phenol	C_6H_6O	0.71	0.76	0.74	0.70
Phenol, 2-methyl-	C_7H_8O	0.59	0.52	0.61	0.54
Phenol, 3-methyl-	C_7H_8O	0.91	0.81	0.81	0.86
Phenol, 2-methoxy-	$C_7H_8O_2$	3.62	3.46	3.45	3.40
Phenol, 2-ethyl-	$C_8H_{10}O$	0.33	0.31	0.32	0.30
Phenol, 3,4-dimethyl-	$C_8H_{10}O$	0.24	0.31	0.31	0.29
Phenol, 2,4-dimethyl-	$C_8H_{10}O$	0.19	0.27	0.29	0.28
Phenol, 4-ethyl-	$C_8H_{10}O$	0.36	0.21	0.30	0.41
Phenol, 3-ethyl-	$C_8H_{10}O$	0.37	0.22	0.29	0.42
Phenol, 2-methoxy-3-methyl-	$C_8H_{10}O_2$	–	–	–	0.15

Table 4 (continued)

Compounds	Molecular formula	Area (%)			
		Fresh	7 days	24 h	168 h
Creosol	$C_8H_{10}O_2$	0.77	0.98	1.00	1.15
1,2-Benzenediol	$C_6H_6O_2$	–	–	–	0.28
Phenol, 4-ethyl-3-methyl-	$C_9H_{12}O$	0.17	0.19	0.24	0.36
Phenol, 4-ethyl-2-methoxy-	$C_9H_{12}O_2$	1.44	1.36	1.53	1.49
2-Methoxy-4-vinylphenol	$C_9H_{10}O_2$	0.70	0.63	0.62	0.51
Phenol, 2,6-dimethoxy-	$C_8H_{10}O_3$	2.59	2.47	2.61	2.47
Phenol, 2-methoxy-4-(1-propenyl)-	$C_{10}H_{12}O_2$	–	–	0.36	0.35
Phenol, 2-methoxy-4-propyl-	$C_{10}H_{14}O_2$	–	0.56	0.59	0.55
Phenol, 2-methoxy-4-(1-propenyl)-	$C_{10}H_{12}O_2$	–	0.33	0.35	0.34
Phenol, 2-methoxy-4-(1-propenyl)-	$C_{10}H_{12}O_2$	1.84	1.63	1.73	1.66
2,6-Dimethoxy-4-vinylphenol	$C_{10}H_{12}O_3$	0.31	0.43	0.41	0.30
Phenol, 2,6-dimethoxy-4-(2-propenyl)-	$C_{11}H_{14}O_3$	–	–	–	0.16
2,6-Dimethoxy-4-propylphenol	$C_{11}H_{16}O_3$	0.34	0.38	0.40	0.37
Phenol, 2,6-dimethoxy-4-(2-propenyl)-	$C_{11}H_{14}O_3$	1.31	1.41	1.23	1.37
Polycyclic aromatic hydrocarbons					
Naphthalene, 1,2,3,4-tetrahydro-2,2,5,7-tetramethyl-	$C_{14}H_{20}$	–	0.27	0.26	0.25

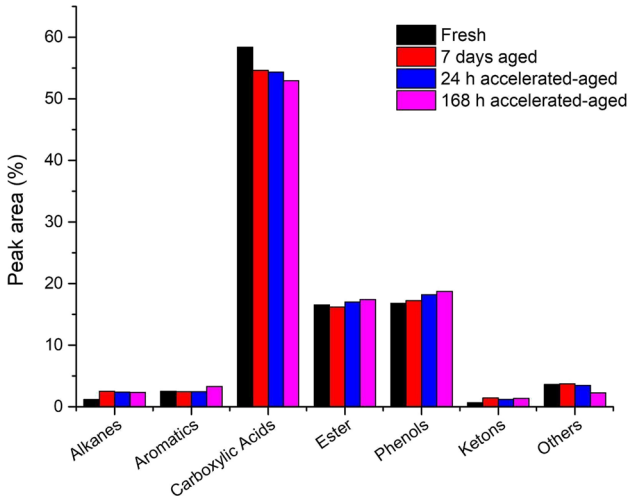

Fig. 3 Relative contents of different groups of chemicals in bio-oil samples before and after the aging process

by a shoulder between approximately 360 and 520 °C. The magnitude of the shoulder increased significantly for the 168-h accelerated aged bio-oil sample due to the same reason explained above. The degradation of higher molecular weight compounds and aromatic structures is more difficult than the simple short-chain hydrocarbons having lower boiling points. After 500 °C, the mass loss rate decreased, and both TG and dTG curves became almost flat. As seen in Table 5, the bio-oil aged for 7 days at room temperature showed a similar decomposition behavior to 168-h accelerated aged bio-oil. On the other hand, decomposition of 24-h accelerated aging was found to be similar to that of fresh sample.

The evolved gases during the thermal decomposition of bio-oil samples were detected via FT-IR spectroscopy at the maximum decomposition temperatures (Table 5), and FT-IR spectra are shown in Fig. 5. Regardless of the storage time, the volatile formation is similar for all samples due to the complex reactions occurring during heat treatment. The thermal composition of bio-oil comprises mainly decarboxylation, dehydration, and depolymerization of high molecular weight, long-chain hydrocarbons, yielding lower molecular weight gas products whose functional groups can be detected via FT-IR. As seen in Fig. 5, the main peak belonging to strong stretching vibrations of O = C = O is observed between 2400 and 2210 cm^{-1}, indicating the presence of carbon dioxide. The sharp peaks of O–H vibrations between 3750 and 3580 cm^{-1} are assigned to the alcohols and observed for mainly the aged samples. During the pyrolysis of bio-oil, the evolution of low molecular weight aliphatics is established by the stretching vibrations of C-H between 3000 and 2840 cm^{-1}, specifically for the fresh bio-oil sample. The C = O stretching band between 1780 and 1735 cm^{-1} is attributed to carboxylic acids and esters. Moreover, the overlapping vibrations of carbonyl and C = C stretching bands between 1850 and 1690 cm^{-1} indicate the release of aldehydes and acids. The weak bands for C-O stretching vibrations (1225–1200 cm^{-1}) are indicative of the formation of ether groups [55]. Since the composition of bio-oil samples slightly changed after the aging process, no detectable difference in the volatile formation was recognized during the decomposition process.

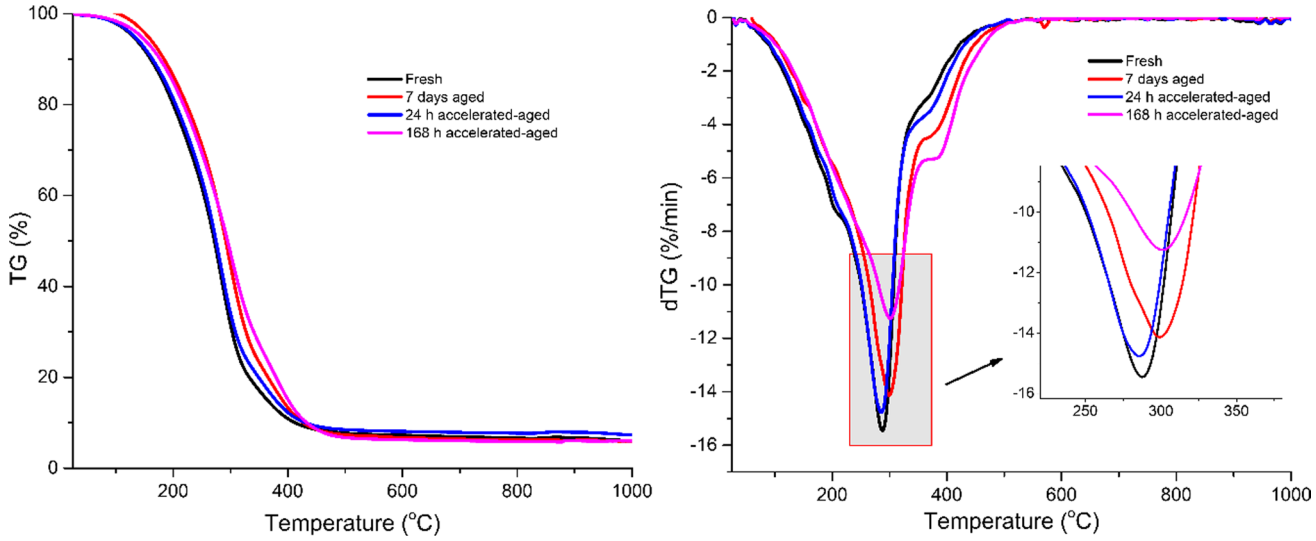

Fig. 4 Thermal decomposition of fresh and aged bio-oil samples: TG and dTG curves

Table 5 Thermal decomposition characteristics of fresh and aged bio-oil samples

Bio-oil	T_i [i]	T_{max} [ii]	T_{sh} [iii]	T_f [iv]	Total mass loss (wt. %)
Fresh	43	281	376	519	93.2
7 days aged	44	295	389	526	94.1
24-h accelerated aged	44	281	380	515	92.5
168-h accelerated aged	46	298	392	518	93.1

[i] T_i, temperature at which the decomposition is started (°C)

[ii] T_{max}, temperature at which the highest decomposition rate is observed (°C)

[iii] T_{sh}, temperature at the shoulder after the main decomposition (°C)

[iv] T_f, temperature at which the decomposition is completed (°C)

3.2.5 Rheological behavior

One of the most important key properties of fuel for the design and operation of processing equipment is viscosity. For instance, a typical liquid fuel injection system is affected by variations in viscosity since the fluidity of the fuel at different temperatures changes significantly [56]. While temperature plays an important role in the viscosity of bio-oil, other factors such as the pyrolysis conditions, raw material, and accordingly the chemical composition of bio-oil are also important factors in the rheological behavior.

The dynamic viscosities of olive pomace bio-oil at different temperatures were measured between the shear rates of 5 and 580 s^{-1} (Fig. 6). The trends observed in the shear

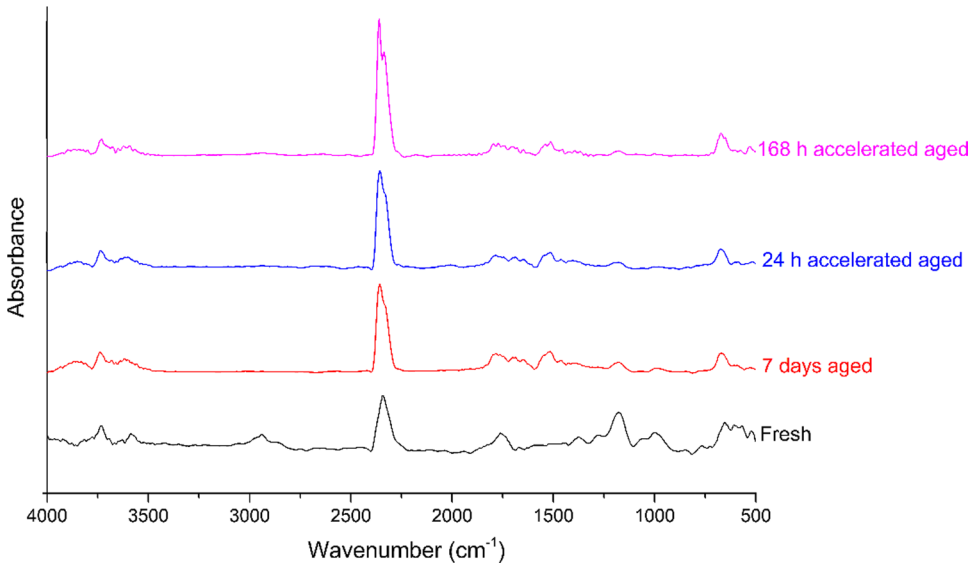

Fig. 5 FT-IR spectra of volatiles evolved during the thermal decomposition of fresh and aged bio-oil samples at the maximum decomposition rate

rate ramp tests appeared to be close to each other for the four bio-oil samples (i.e., fresh, 7-day aged, 24-h accelerated aged, and 168-h accelerated aged). Aged bio-oil samples exhibited qualitatively similar viscosity-shear rate response to the fresh bio-oil sample that has the lowest mean dynamic viscosities at all temperatures. According to Nolte et al., at temperatures lower than 55 °C, most bio-oil samples behave as Newtonian fluids [57]. In this study, the dynamic viscosity was almost constant at a broad range of shear rates (5–580 s^{-1}). However, all samples at all temperatures began to shear thickening at around 200 s^{-1}; therefore, the average viscosity was calculated at a shear rate between 10 and 50 s^{-1}, where the dynamic viscosity was almost constant. Table 6 represents the viscosities of fresh and aged bio-oil samples at different temperatures, along with the calculated aging indexes (AI). The fresh bio-oil sample exhibited the lowest viscosity values at all temperatures, whereas the 168-h accelerated aged bio-oil had the highest viscosity. In general, the viscosity of fresh and aged bio-oil samples produced from olive pomace decreased when the temperature increased. A similar trend was reported for several bio-oils produced by fast or slow pyrolysis at different final temperatures from different biomasses such as rice husk [58],

Table 6 Viscosity (η; cP) and aging index (AI; %) of fresh and aged bio-oil samples

Temperature		Fresh	7-day aged	24-h accelerated aging	168-h accelerated aging
20 ℃	η	75.7	84.7	89.4	111.2
	AI	-	11.8	18.0	46.8
25 ℃	η	57.9	65.3	67.8	82.4
	AI	-	12.9	17.3	42.33
30 ℃	η	45.3	51.9	52.6	63.5
	AI	-	14.5	16.0	40.1
35 ℃	η	36.3	42.2	41.7	50.2
	AI	-	16.1	14.9	38.2
40℃	η	29.8	34.9	33.9	40.7
	AI	-	17.0	13.7	36.5

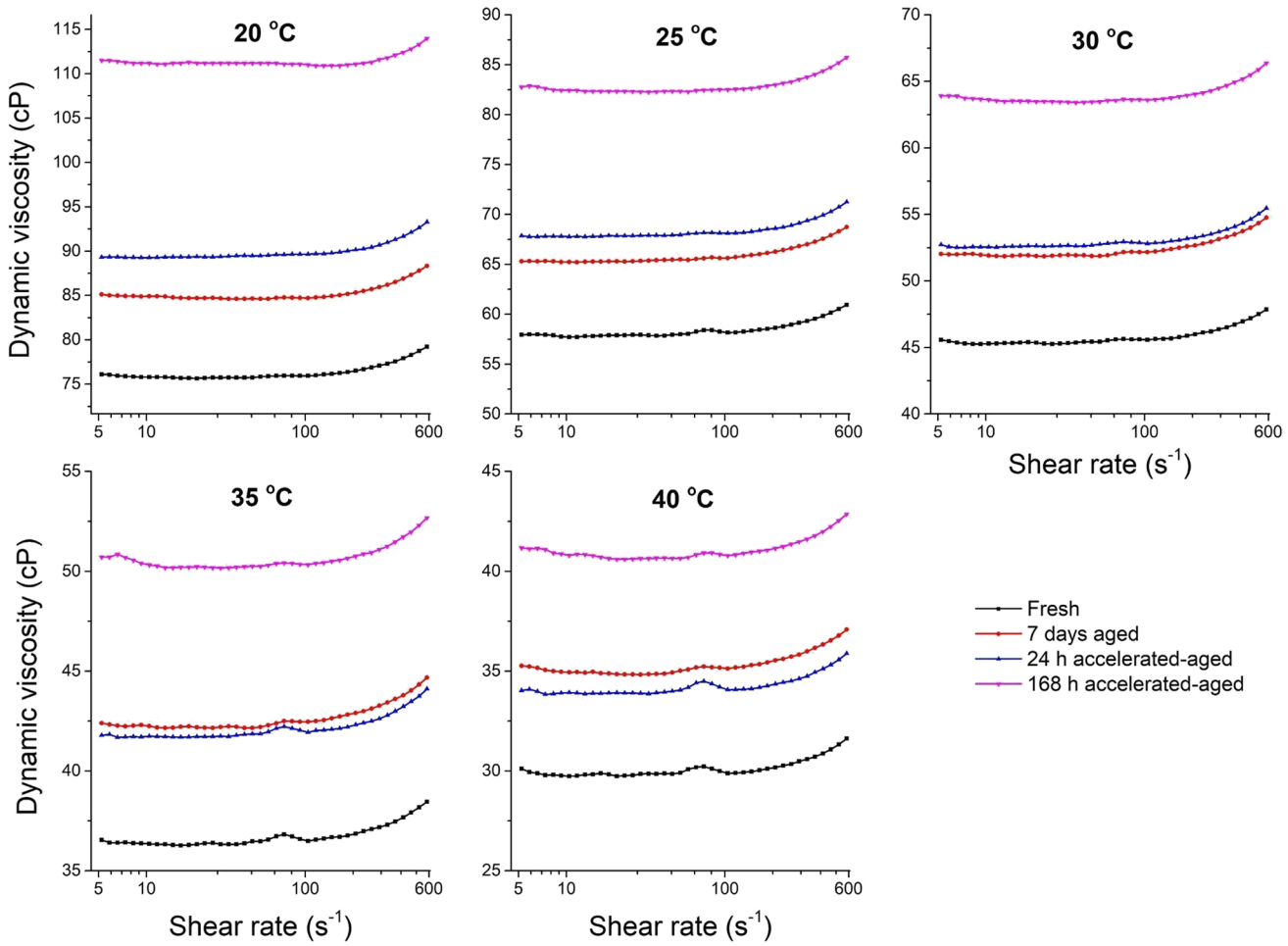

Fig. 6 Viscosity vs shear rate at different temperatures

pinewood [59], softwood bark [60], walnut shell flour [61], and greenhouse crop residue [62].

The viscosity of fresh and aged bio-oil samples, given in Table 6, was found to be within the range of typical bio-oil viscosities (40–120 cP, at 50 °C) reported previously and lower than the heavy fuel oil viscosity of 180 cP [63]. The viscosity of fresh bio-oil showed a decrease of approximately 60% when the temperature increased from 20 to 40 °C. A similar decrement of 60 ± 3% was achieved for the aged bio-oil samples. The viscosity of 7 days aged sample was 5.5% higher than that of fresh bio-oil, whereas the viscosity of the 168-h accelerated aged bio-oil sample was reported as 111.2 cP. The calculated aging indexes for both natural and accelerated aged samples are also listed in Table 6. The effect of accelerated aging on bio-oil is seen in the aging indexes. The aging index values were calculated as 11.9, 12.9, 14.5, 16.1, and 17.0% at the five different temperatures between 20 and 40 °C for the 7-day naturally aged bio-oil. On the other hand, the aging indexes were 46.8, 42.3, 40.1, 38.2, and 36.5% for bio-oil samples stored at 80 °C for the same duration (7 days) at the same temperature ranges. Storing bio-oil at room temperature had a lower effect on the viscosity at lower temperatures (20, 25, and 30 °C), while the viscosity at higher temperatures (35 and 40 °C) exhibited a higher effect.

Generally, the temperature has a significant effect on the dynamic viscosity, as the temperature increase, the dynamic viscosity decreases. Moreover, it is seen that the temperature has a higher effect on the accelerated aged samples compared to the aged sample at room temperature. At relatively higher temperatures (35 and 40 °C), the dynamic viscosity of 24-h accelerated aged sample was recorded to be lower than 7-day aged sample at room temperature. The results showed that storing bio-oil at room temperature for 7 days had a similar effect as 24 h accelerated aging.

At the shear rates between 5 and 580 s^{-1}, fresh and aged bio-oil samples followed Newton's law of viscosity with the linear relationship between the shear stress and the shear rate as shown in Fig. 7. The slope of the straight lines refers to the constant viscosity that is independent of the shear rate. The viscosity remained constant at different shear rates for each sample for all temperatures. The aging process did not affect the rheological behavior of the bio-oil. Experimental data fit the Newtonian model very well with R^2 values higher than 0.99 for all samples at all measured temperatures.

The relationship between viscosity (η) and temperature can be demonstrated by the Arrhenius equation as given as follows:

$$\eta = Ae^{\frac{E}{RT}} \tag{3}$$

where η is the dynamic viscosity of bio-oil; A is a constant (cP); E represents the flow activation energy; and R is the universal gas constant (8.314 $J.mol^{-1}.K^{-1}$) [59]. To achieve a linear relationship between viscosity and temperature, the Arrhenius equation is linearized as in Eq. 4 [57]:

$$ln\eta = lnA + \frac{E}{RT} \tag{4}$$

Equation 4 can be plotted as a straight line with $ln(\eta)$ versus $1000/T$ (Fig. 8). The values of E which is related to the rate of vaporization of the bio-oil were calculated from the slope of the straight lines and given in Table 7. The flow activation energies of all bio-oil samples are similar at around 40 $kJ.mol^{-1}$, which is close to that of bio-oil produced from pinewood [59], lower than that of oak and poplar wood bio-oils [64], and higher than that of water and gasoline [57]. The activation energy was slightly decreased after the aging process. This could be due to esterification and acetalization reactions that occurred during the aging period to form ester, acetyls, and water as products.

4 Conclusions

The thermal stability of bio-oil is an important property as bio-oil might be exposed to different temperatures during storage life. The detailed information on the effect of

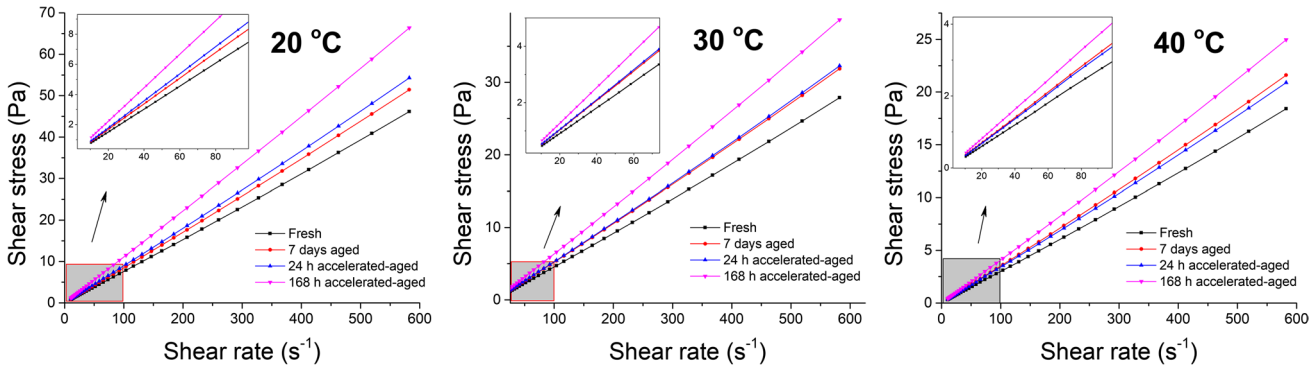

Fig. 7 Shear stress versus shear rate of fresh and aged bio-oil samples at 20, 30, and 40 °C

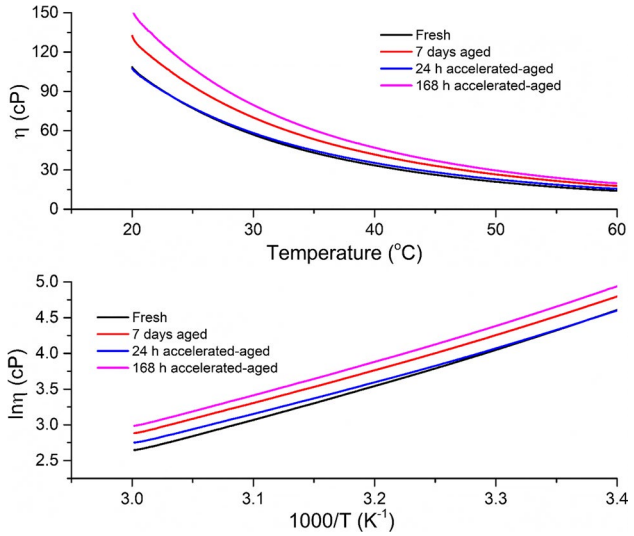

Fig. 8 Arrhenius plot of fresh and aged bio-oil samples

temperature on bio-oil can lead to better storage conditions. Also, the storage stability of bio-fuel should be high enough to consider it as an alternative fuel.

The compositional, thermal, and rheological characteristics of the bio-oil were studied to evaluate its stability during storage. The bio-oil samples produced from olive pomace were aged at room temperature for 7 days and at 80 °C for 24 and 168 h. The thermal stability tests revealed the fact that the decomposition of bio-oil shifted to higher temperatures after the aging process since the higher molecular weight hydrocarbons present in the bio-oil were retained during the storage conditions, while the lower molecular weight compounds volatilized. Also, carbon dioxide, carboxylic acids, and aliphatics were detected as the evolved gases during the thermal decomposition via simultaneous FT-IR. The influence of aging on bio-oil rheology was examined through the viscosities at different temperatures. The viscosity of bio-oil increased from 29.8 (fresh) to 40.7 cP (168-h accelerated aged) at 40 °C due to the possible polymerization, decarboxylation, esterification, and dehydrogenation reactions that occurred during storage which resulted in a significant change in the chemical composition. According to GC–MS results, carboxylic acid (mainly oleic acid, 46.8% of bio-oil) content decreased, while the new formation of esters was observed.

Table 7 Arrhenius coefficients and activation energies of fresh and aged bio-oil samples

Bio-oil	A (cP)	E/R	R^2	E (kJ.mol^{-1})
Fresh	4.76×10^{-6}	4.94	0.9982	41.11
7-day aged	9.68×10^{-6}	4.79	0.9984	39.84
24-h accelerated aging	1.29×10^{-5}	4.65	0.9980	38.65
168-h accelerated aging	8.01×10^{-6}	4.89	0.9983	40.63

As a result, understanding the effects of storage on bio-oil may lead to new investigations on the methods to increase the stability and quality of bio-oil, which will accelerate the commercial use of this renewable and environmentally friendly energy source. Besides, the outcome of this study will make it possible to understand structural, thermal, and rheological changes taking place with aging, which in turn, helps develop more feasible biorefinery processes. For future works, the aging effects using different upgrading methods could be analyzed in terms of characterization and rheological behavior of olive pomace-based bio-oil. Furthermore, the exact accelerated aging effects on the viscosity compared to long-term temperature aging may be investigated.

Acknowledgements This paper is dedicated to our dear colleague Prof. Dr. Başak Burcu Uzun, who tragically deceased during the completion of this project.

Author contribution **Ahmed Ayyash:** conceptualization, investigation, writing—original draft.

Esin Apaydın Varol: conceptualizing, writing—review and editing, supervision.

Murat Kılıç: funding acquisition, resources, writing—review and editing.

Gamzenur Özsin: resources, visualization, writing—review and editing.

Funding The research leading to these results received funding from Anadolu University Scientific Research Projects Unit under Grant Agreement No. 1506F496.

Declarations

Competing Interests The authors declare no competing interests.

References

1. Mehmood MA, Ahmad MS, Liu Q, Liu C-G, Tahir MH, Alo-qbi AA, Tarbiah NI, Alsufiani HM, Gull M (2019) Helianthus tuberosus as a promising feedstock for bioenergy and chemicals appraised through pyrolysis, kinetics, and TG-FTIR-MS based study. Energy Convers Manage 194:37–45. https://doi.org/10.1016/j.enconman.2019.04.076
2. J. Li, K.G. Burra, Z. Wang, X. Liu, A.K. Gupta, Effect of alkali and alkaline metals on gas formation behavior and kinetics during pyrolysis of pine wood, Fuel 290 (2021). https://doi.org/10.1016/j.fuel.2020.120081
3. Ontyd C, Pielsticker S, Yildiz C, Schiemann M, Hatzfeld O, Ströhle J, Epple B, Kneer R, Scherer V (2021) Experimental determination of walnut shell pyrolysis kinetics in N2 and CO2 via thermogravimetric analysis, fluidized bed and drop tube reactors. Fuel 287:119313. https://doi.org/10.1016/j.fuel.2020.119313

4. Bridgwater AV (2012) Review of fast pyrolysis of biomass and product upgrading. Biomass Bioenerg 38:68–94. https://doi.org/10.1016/j.biombioe.2011.01.048
5. Amjith LR, Bavanish B (2022) A review on biomass and wind as renewable energy for sustainable environment. Chemosphere 293:133579. https://doi.org/10.1016/j.chemosphere.2022.133579
6. A.K. Agarwal, R.A. Agarwal, T. Gupta, B.R. Gurjar, Introduction to biofuels, in: A.K. Agarwal, R.A. Agarwal, T. Gupta, B.R. Gurjar (Eds.), Biofuels: technology, challenges and prospects, Springer Singapore, Singapore, 2017, pp. 3–6. https://doi.org/10.1007/978-981-10-3791-7_1
7. Tahir MH, Çakman G, Goldfarb JL, Topcu Y, Naqvi SR, Ceylan S (2019) Demonstrating the suitability of canola residue biomass to biofuel conversion via pyrolysis through reaction kinetics, thermodynamics and evolved gas analyses. Biores Technol 279:67–73. https://doi.org/10.1016/j.biortech.2019.01.106
8. F. Rego, H. Xiang, Y. Yang, J.L. Ordovás, K. Chong, J. Wang, A. Bridgwater, Investigation of the role of feedstock properties and process conditions on the slow pyrolysis of biomass in a continuous auger reactor, Journal of Analytical and Applied Pyrolysis 161 (2022). https://doi.org/10.1016/j.jaap.2021.105378
9. Ghouma I, Jeguirim M, Guizani C, Ouederni A, L. (2017) Limousy. Pyrolysis of olive pomace: degradation kinetics, gaseous analysis and char characterization, waste and biomass valorization 8(5):1689–1697. https://doi.org/10.1007/s12649-017-9919-8
10. Ahmad MS, Klemeš JJ, Alhumade H, Elkamel A, Mahmood A, Shen B, Ibrahim M, Mukhtar A, Saqib S, Asif S, Bokhari A (2021) Thermo-kinetic study to elucidate the bioenergy potential of maple leaf waste (MLW) by pyrolysis. TGA and kinetic modelling, Fuel 293:120349. https://doi.org/10.1016/j.fuel.2021.120349
11. 2019 Yılı Zeytin ve Zeytinyağı Raporu, Turkiye, 2020
12. Ruiz E, Romero-García JM, Romero I, Manzanares P, Negro MJ, Castro E (2017) Olive-derived biomass as a source of energy and chemicals. Biofuels, Bioprod Biorefin 11(6):1077–1094. https://doi.org/10.1002/bbb.1812
13. Parascanu MM, PuigGamero M, Sánchez P, Soreanu G, Valverde JL, Sanchez-Silva L (2018) Life cycle assessment of olive pomace valorisation through pyrolysis. Renewable Energy 122:589–601. https://doi.org/10.1016/j.renene.2018.02.027
14. Dinc G, Yel E (2020) Alternative approach for safe disposal of dry olive pomace: pyrolysis with/without physical preprocessing. Int J Environ Sci Technol 17(4):2215–2232. https://doi.org/10.1007/s13762-019-02612-z
15. A.-L. Skaltsounis, A. Argyropoulou, N. Aligiannis, N. Xynos, 11 - Recovery of high added value compounds from olive tree products and olive processing byproducts, in: D. Boskou (Ed.), Olive and Olive Oil Bioactive Constituents, AOCS Press2015, pp. 333–356. https://doi.org/10.1016/B978-1-63067-041-2.50017-3
16. Uzun BB, Pütün AE, Pütün E (2007) Rapid pyrolysis of olive residue 1 Effect of heat and mass transfer limitations on product yields and bio-oil compositions. Energy & Fuels 21(3):1768–1776. https://doi.org/10.1021/ef060171a
17. H. Cay, G. Duman, G. Balmuk, I.C. Kantarli, J. Yanik, Impact of carbonization on the combustion and gasification reactivities of olive wastes, Green Energy Technol (2020) 323–343. https://doi.org/10.1007/978-3-030-20637-6_18
18. A. Gálvez-Pérez, M.A. Martín-Lara, M. Calero, A. Pérez, P. Canu, G. Blázquez, Experimental investigation on the air gasification of olive cake at low temperatures, Fuel Processing Technology 213 (2021). https://doi.org/10.1016/j.fuproc.2020.106703
19. E.T. Kostas, G. Durán-Jiménez, B.J. Shepherd, W. Meredith, L.A. Stevens, O.S.A. Williams, G.J. Lye, J.P. Robinson, Microwave pyrolysis of olive pomace for bio-oil and bio-char production, Chemical Engineering Journal 387 (2020). https://doi.org/10.1016/j.cej.2019.123404
20. Pütün AE, Uzun BB, Apaydin E, Pütün E (2005) Bio-oil from olive oil industry wastes: pyrolysis of olive residue under different conditions. Fuel Process Technol 87(1):25–32. https://doi.org/10.1016/j.fuproc.2005.04.003
21. Uzun BB, Pütün AE, Pütün E (2007) Composition of products obtained via fast pyrolysis of olive-oil residue: effect of pyrolysis temperature. J Anal Appl Pyrol 79(1–2):147–153. https://doi.org/10.1016/j.jaap.2006.12.005
22. Pütün E, Uzun BB, Pütün AE (2009) Rapid pyrolysis of olive residue 2 Effect of catalytic upgrading of pyrolysis vapors in a two-stage fixed-bed reactor. Energy & Fuels 23(4):2248–2258. https://doi.org/10.1021/ef800978m
23. Alcazar-Ruiz A, Ortiz ML, Sanchez-Silva L, Dorado F (2021) Catalytic effect of alkali and alkaline earth metals on fast pyrolysis pre-treatment of agricultural waste. Biofuels, Bioprod Biorefin 15(5):1473–1484. https://doi.org/10.1002/bbb.2253
24. Wang S, Luo Z (2016). De Gruyter. https://doi.org/10.1515/9783110369632
25. A.T. Hoang, H.C. Ong, I.M.R. Fattah, C.T. Chong, C.K. Cheng, R. Sakthivel, Y.S. Ok, Progress on the lignocellulosic biomass pyrolysis for biofuel production toward environmental sustainability, Fuel Processing Technology 223 (2021). https://doi.org/10.1016/j.fuproc.2021.106997
26. Djokic MR, Dijkmans T, Yildiz G, Prins W, Van Geem KM (2012) Quantitative analysis of crude and stabilized bio-oils by comprehensive two-dimensional gas-chromatography. J Chromatogr A 1257:131–140. https://doi.org/10.1016/j.chroma.2012.07.035
27. W. Cai, N. Kang, M.K. Jang, C. Sun, R. Liu, Z. Luo, Long term storage stability of bio-oil from rice husk fast pyrolysis, Energy 186 (2019). https://doi.org/10.1016/j.energy.2019.115882
28. W. Yi, X. Wang, K. Zeng, H. Yang, J. Shao, S. Zhang, H. Chen, Improving bio-oil stability by fractional condensation and solvent addition, Fuel 290 (2021). https://doi.org/10.1016/j.fuel.2020.119929
29. KhosravanipourMostafazadeh A, Solomatnikova O, Drogui P, Tyagi RD (2018) A review of recent research and developments in fast pyrolysis and bio-oil upgrading. Biomass Conversion and Biorefinery 8(3):739–773. https://doi.org/10.1007/s13399-018-0320-z
30. Elliott DC, Oasmaa A, Meier D, Preto F, Bridgwater AV (2012) Results of the IEA round robin on viscosity and aging of fast pyrolysis bio-oils: long-term tests and repeatability. Energy Fuels 26(12):7362–7366. https://doi.org/10.1021/ef301607v
31. Chen D, Zhou J, Zhang Q, Zhu X (2014) Evaluation methods and research progresses in bio-oil storage stability. Renew Sustain Energy Rev 40:69–79. https://doi.org/10.1016/j.rser.2014.07.159
32. Elorf A, Kandasamy J, Belandria V, Bostyn S, Sarh B, Gökalp I (2021) Heating rate effects on pyrolysis, gasification and combustion of olive waste. Biofuels 12(9):1157–1164. https://doi.org/10.1080/17597269.2019.1594598
34. Dorado F, Sanchez P, Alcazar-Ruiz A, Sanchez-Silva L (2021) Fast pyrolysis as an alternative to the valorization of olive mill wastes. J Sci Food Agric 101(7):2650–2658. https://doi.org/10.1002/jsfa.10856
35. Dinc G, Yel E (2018) Self-catalyzing pyrolysis of olive pomace. J Anal Appl Pyrol 134:641–646. https://doi.org/10.1016/j.jaap.2018.08.018
36. Encinar JM, González JF, Martínez G, Román S (2009) Catalytic pyrolysis of exhausted olive oil waste. J Anal Appl Pyrol 85(1):197–203. https://doi.org/10.1016/j.jaap.2008.11.018
37. Manyà JJ, Alvira D, Azuara M, Bernin D, Hedin N (2016) Effects of pressure and the addition of a rejected material from municipal waste composting on the pyrolysis of two-phase olive mill waste.

Energy Fuels 30(10):8055–8064. https://doi.org/10.1021/acs.energyfuels.6b01579
38. Manyà JJ, Laguarta S, Ortigosa MA, Manso JA (2014) Biochar from slow pyrolysis of two-phase olive mill waste: effect of pressure and peak temperature on its potential stability. Energy Fuels 28(5):3271–3280. https://doi.org/10.1021/ef500654t
39. Dinc G, Yel E (2020) Comparative study of olive pomace pyrolysis with/without ultrasonic preprocessing. Int J Environ Sci Technol 17(5):2511–2528. https://doi.org/10.1007/s13762-019-02608-9
40. J.P. Diebold, A review of the chemical and physical mechanisms of the storage stability of fast pyrolysis biooil, 2000
41. Meng J, Moore A, Tilotta DC, Kelley SS, Adhikari S, Park S (2015) Thermal and storage stability of bio-oil from pyrolysis of torrefied wood. Energy Fuels 29(8):5117–5126. https://doi.org/10.1021/acs.energyfuels.5b00929
42. Özsin G, Pütün AE (2018) A comparative study on co-pyrolysis of lignocellulosic biomass with polyethylene terephthalate, polystyrene, and polyvinyl chloride: synergistic effects and product characteristics. J Clean Prod 205:1127–1138. https://doi.org/10.1016/j.jclepro.2018.09.134
43. Hilten RN, Das KC (2010) Comparison of three accelerated aging procedures to assess bio-oil stability. Fuel 89(10):2741–2749. https://doi.org/10.1016/j.fuel.2010.03.033
44. Meng J, Park J, Tilotta D, Park S (2012) The effect of torrefaction on the chemistry of fast-pyrolysis bio-oil. Bioresour Technol 111:439–446. https://doi.org/10.1016/j.biortech.2012.01.159
45. S. Sensoz, I. Demiral, H. Ferdi Gercel, Olive bagasse (Olea europaea L.) pyrolysis, Bioresour Technol 97(3) (2006) 429–36. https://doi.org/10.1016/j.biortech.2005.03.007
46. Cheng T, Han Y, Zhang Y, Xu C (2016) Molecular composition of oxygenated compounds in fast pyrolysis bio-oil and its supercritical fluid extracts. Fuel 172:49–57. https://doi.org/10.1016/j.fuel.2015.12.075
47. Mante OD, Agblevor FA (2012) Storage stability of biocrude oils from fast pyrolysis of poultry litter. Waste Manag 32(1):67–76. https://doi.org/10.1016/j.wasman.2011.09.004
48. B. Viswanathan, Petroleum, Energy Sources2017, pp. 29–57. https://doi.org/10.1016/b978-0-444-56353-8.00002-2
49. Kit Ling C, H.n. Paik San, E. HooiKyin, L. Seng Hua, L. Wei Chen, C. Yin Yee, (2015) Yield and calorific value of bio oil pyrolysed from oil palm biomass and its relation with solid residence time and process temperature. Asian Journal of Scientific Research 8(3):351–358. https://doi.org/10.3923/ajsr.2015.351.358
50. Tucureanu V, Matei A, Avram AM (2016) FTIR spectroscopy for carbon family study. Crit Rev Anal Chem 46(6):502–520. https://doi.org/10.1080/10408347.2016.1157013
51. Grioui N, Halouani K, Agblevor FA (2014) Bio-oil from pyrolysis of Tunisian almond shell: comparative study and investigation of aging effect during long storage. Energy Sustain Dev 21:100–112. https://doi.org/10.1016/j.esd.2014.05.006
52. Sahoo A, Kumar S, Mohanty K (2020) A comprehensive characterization of non-edible lignocellulosic biomass to elucidate their biofuel production potential. Biomass Conversion and Biorefinery. https://doi.org/10.1007/s13399-020-00924-6
53. Uzun BB, Apaydin-Varol E, Ateş F, Özbay N, Pütün AE (2010) Synthetic fuel production from tea waste: characterisation of bio-oil and bio-char. Fuel 89(1):176–184. https://doi.org/10.1016/j.fuel.2009.08.040
54. D.T.d. Almeida, T.V. Viana, M.M. Costa, C.d.S. Silva, S. Feitosa, Effects of different storage conditions on the oxidative stability of crude and refined palm oil, olein and stearin (Elaeis guineensis), Food Science and Technology 39(suppl 1) (2019) 211–217. https://doi.org/10.1590/fst.43317
55. M.H. Tahir, X. Cheng, R.M. Irfan, R. Ashraf, Y. Zhang, Comparative chemical analysis of pyrolyzed bio oil using online TGA-FTIR and GC-MS, Journal of Analytical and Applied Pyrolysis 150 (2020). https://doi.org/10.1016/j.jaap.2020.104890
56. Lu Q, Yang X-L, Zhu X-F (2008) Analysis on chemical and physical properties of bio-oil pyrolyzed from rice husk. J Anal Appl Pyrol 82(2):191–198. https://doi.org/10.1016/j.jaap.2008.03.003
57. Nolte MW, Liberatore MW (2010) Viscosity of biomass pyrolysis oils from various feedstocks. Energy Fuels 24(12):6601–6608. https://doi.org/10.1021/ef101173r
58. Zheng J-L, Kong Y-P (2010) Spray combustion properties of fast pyrolysis bio-oil produced from rice husk. Energy Convers Manage 51(1):182–188. https://doi.org/10.1016/j.enconman.2009.09.010
59. Thangalazhy-Gopakumar S, Adhikari S, Ravindran H, Gupta RB, Fasina O, Tu M, Fernando SD (2010) Physiochemical properties of bio-oil produced at various temperatures from pine wood using an auger reactor. Bioresour Technol 101(21):8389–8395. https://doi.org/10.1016/j.biortech.2010.05.040
60. Moutsoglou A, Lawburgh B, Lawburgh J (2018) Fractional condensation and aging of pyrolysis oil from softwood and organosolv lignin. J Anal Appl Pyrol 135:350–360. https://doi.org/10.1016/j.jaap.2018.08.016
61. H. Ding, C. Wang, X. Zhu, Estimation of the kinematic viscosities of bio-oil/alcohol blends: kinematic viscosity-temperature formula and mixing rules, Fuel 254 (2019). https://doi.org/10.1016/j.fuel.2019.115687
62. I. Iáñez-Rodríguez, M.A. Martín-Lara, G. Blázquez, M. Calero, Effect of different pre-treatments and addition of plastic on the properties of bio-oil obtained by pyrolysis of greenhouse crop residue, Journal of Analytical and Applied Pyrolysis 153 (2021). https://doi.org/10.1016/j.jaap.2020.104977
63. C.U.P. Dinesh Mohan, Philip H. Steele, Pyrolysis of wood/biomass for bio-oil: a critical review, Energy and Fuels 20 (2006)
64. Leroy J, Choplin L, Kaliaguine S (1988) Rheological characterization of pyrolytic wood derived oils: existence of a compensation effect. Chem Eng Commun 71(1):157–176. https://doi.org/10.1080/00986448808940421